Peroxinredoxin 6 reduction accelerates cigarette smoke extract-induced senescence by regulating autophagy in BEAS-2B cells

JINLONG LUO, XIAOCEN WANG, TINGTING WEI, KE LANG, CHEN BAO and DONG YANG

Department of Pulmonary Medicine, Zhongshan Hospital, Fudan University, Shanghai 200032, P.R. China

Received December 10, 2022; Accepted May 24, 2023

DOI: 10.3892/etm.2023.12074

Abstract. Cigarette smoke (CS)-induced accelerated senescence and insufficient autophagy has been implicated in the pathogenesis of chronic obstructive pulmonary disease (COPD). Peroxiredoxin (PRDX) 6 is a protein with prevalent antioxidant capacity. Previous studies indicate that PRDX6 could activate autophagy and alleviate senescence in other diseases. The present study investigated whether PRDX6-regulated autophagy was involved in the regulation of CS extract (CSE)-induced BEAS-2B cell senescence via the knockdown of PRDX6 expression. Furthermore, the present study evaluated the mRNA levels of PRDX6, autophagy and senescence-associated genes in the small airway epithelium from patients with COPD by analyzing the GSE20257 dataset from the Gene Expression Omnibus database. The results demonstrated that CSE reduced PRDX6 expression levels and transiently induced the activation of autophagy, followed by the accelerated senescence of BEAS-2B cells. Knockdown of PRDX6 induced autophagy degradation and accelerated senescence in CSE-treated BEAS-2B cells. Furthermore, autophagy inhibition by 3-Methyladenine increased P16 and P21 expression levels, while autophagy activation by rapamycin reduced P16 and P21 expression levels in CSE-treated BEAS-2B cells. The GSE20257 dataset revealed that patients with COPD had lower PRDX6, sirtuin (SIRT) 1 and SIRT6 mRNA levels, and higher P62 and P16 mRNA levels compared with non-smokers. P62 mRNA was significantly correlated with P16, P21 and SIRT1, which indicated that insufficient autophagic clearance of damaged proteins could be involved in accelerated cell senescence in COPD. In conclusion, the present study demonstrated a novel protective role for PRDX6 in COPD. Furthermore, a reduction in PRDX6 could accelerate senescence by inducing autophagy impairment in CSE-treated BEAS-2B cells.

Correspondence to: Professor Dong Yang, Department of Pulmonary Medicine, Zhongshan Hospital, Fudan University, 180 Fenglin Road, Shanghai 200032, P.R. China
E-mail: yang.dong@zs-hospital.sh.cn

Key words: chronic obstructive pulmonary disease, peroxiredoxin 6, autophagy, senescence, cigarette smoke extract

Introduction

Chronic obstructive pulmonary disease (COPD) is one of the most common chronic diseases worldwide. With 212.3 million prevalent cases and 16.2 million new cases, COPD accounted for 3.3 million deaths globally in 2019 (1). Cigarette smoking is the main and most common risk factor for COPD (2). Cigarette smoking induces the production of reactive oxygen species (ROS) and oxidative stress in the epithelium of the airway and lungs. Exposure to cigarette smoke (CS) leads to airway epithelium injury and phenotypic changes, such as mitochondrial dysfunction and cellular senescence, which are the core phenotypes of aging (3,4).

Aging is now considered to be widely implicated in the pathogenesis of COPD (5). Accelerated cell senescence confers COPD progression by impairing cell proliferation and prolonging inflammation partly through the secretion of senescence-associated secretory phenotype factors (e.g., Interleukins like IL-6 and IL-13, Chemokines like IL-8 and MCP-2, and Growth factors or regulators such as VEGF and IGFBP-3) (5,6). Oxidative stress, such as from ROS, is a stressful stimuli that enhances senescence (7). Furthermore, insufficient removal of damaged proteins and organelles, including via dysfunction of the proteasome and autophagy, has been proposed to play a pivotal role in the regulation of cell senescence (8).

Peroxiredoxin (PRDX) is a protein family with a high-efficiency antioxidant capacity (9). As phospholipid hydroperoxidases, PRDXs are abundant in alveolar type II epithelial cells and Clara cells (10). Compared with other PRDX family members, in addition to oxidase activity, PRDX6 has phospholipase A2 activity and can regulate the intracellular oxidation-antioxidation balance by scavenging hydrogen peroxide (H_2O_2), aliphatic and aromatic hydroperoxides, peroxynitrite and peroxidized phospholipids, thereby reducing oxidative stress-induced injury (11). Previous studies have demonstrated that PRDX6 may play a key role in the crosstalk between aging and diseases (12,13). In glaucoma, PRDX6 levels decrease with age and decrease markedly in glaucomatous and aged trabecular meshwork cells. Human trabecular meshwork cells display typical features of oxidative-stress-induced cellular changes, exhibiting increased levels of lipid peroxidation, oxidative DNA damage and senescence markers such as P16, P21 and senescence-associated β-galactosidase

(SA-β-gal) activity (12). Knocking down of PRDX6 expression accelerates this process, while PRDX6 delivery to trabecular meshwork cells reverses the process (12). In diabetic sarcopenia mice, PRDX6 knock out revealed a reduction in telomere length, sirtuin (SIRT) 1 nuclear localization and increased activity in SA-β-Gal and the P53-P21 pro-aging pathway (13). Furthermore, PRDX6 has also been revealed to play a key role in disease progression through regulating mitophagy (14,15). In the study of non-alcoholic fatty liver disease, oxidative stress-induced Notch signaling and lipogenesis were suppressed in PRDX6 overexpressing mice, compared with wild-type mice, through the induction of mitophagy, while PRDX6 knockdown reduced this induction of mitophagy (14). Another study demonstrated that ROS induce the recruitment of PRDX6 to the mitochondria, where PRDX6 controls ROS homeostasis in the initial step of PTEN-induced kinase 1 (PINK1)-Parkin-mediated mitophagy (15). Collectively, these results indicate that PRDX6 may play a key role in senescence and autophagy. However, to the best of our knowledge, there is no research to date that considers the role of PRDX6 on senescence in COPD.

In the present study, we hypothesized that CS reduces the level of PRDX6 in the airway epithelium of patients with COPD. This reduction in PRDX6 then accelerates CS extract (CSE)-induced cellular senescence, at least partly through impairing autophagy.

Materials and methods

CSE preparation. To mimic cigarette smoking-induced injury, CSE was prepared using commercial cigarettes (Daqianmen). Briefly, the smoke of one commercial cigarette was pumped into 10 ml PBS (cat. no. BL302A; Biosharp Life Sciences) using a BT-100-2J peristaltic pump (cat. no. 05.02.11A; Longer Precision Pump Co., Ltd.; Halma plc) to generate a CSE solution. The CSE solution was filtered through a 0.22 μm-pore filter (cat. no. 8160; Corning, Inc.) to remove bacteria and large particles. The CSE solution was then adjusted to pH 7.4 with sodium hydroxide and used within 30 min of preparation. This solution was defined to be 100% CSE, which was diluted in each experiment to obtain the desired concentration.

Cell culture and cell viability. The human bronchial epithelial cell line, BEAS-2B, was obtained and authenticated by STR (iCell Bioscience Inc.; cat. no. iCell-h023) and was cultured at 37˚C with 5% CO_2 in DMEM (cat. no. 11965092; Gibco; Thermo Fisher Scientific, Inc.) supplemented with 10% fetal bovine serum (cat. no. 11573397; Gibco; Thermo Fisher Scientific, Inc.) and 1% penicillin-streptomycin solution (cat. no. 15140122; Gibco; Thermo Fisher Scientific, Inc.). BEAS-2B cells were treated using CSE with/without 5 nM rapamycin (cat. no. R817296; Shanghai Macklin Biochemical Co., Ltd.) or 5 mM 3-methyladenine (3-MA; cat. no. HY-19312, Selleck Chemicals) when the cells reached 80% confluency. Cell viability was determined using the Cell Counting Kit-8 (CCK-8) assay and the Lactate Dehydrogenase (LDH) Cytotoxicity Assay kit (cat. nos. C0037 and C0016, respectively; Beyotime Institute of Biotechnology) following the manufacturer's protocols. Briefly, BEAS-2B cells were seeded in 96-well plates at a density of $1x10^4$ cells/well and stabilized overnight, followed by CSE treatment. Next, 20 μl of CCK-8 or LDH reagent was added to each well of the 96-well plates and incubated for 1 h at 37˚C. The optical density at 450 nm for CCK-8 and 490 nm for LDH reagent were measured using a Microplate Reader (cat. no. 1410101; Thermo Fisher Scientific, Inc.).

Small interfering RNA (siRNA) and transfection. The siRNA targeting PRDX6 and non-targeting negative control siRNA (NC) were purchased from Shanghai GenePharma Co., Ltd. The three siRNA oligonucleotide sequences targeting PRDX6 were as follows: Sequence 1 (S1; PRDX6-Homo-233) sense, 5'-GCCAAGAGGAAUGUUAAGUTT-3' and antisense, 5'-ACUUAACAUUCCUCUUGGCTT-3'; sequence 2 (S2), sense (PRDX6-Homo-513): 5'-GGAACUUUGAUGAGAUUCUTT-3', antisense (PRDX6-Homo-513): 5'-AGAAUCUCAUCAAAGUUCCTT-3'; sequence3, (S3), sense (PRDX6-Homo-301): 5'-GGAUAUCAAUGCUUACAAUTT-3', antisense (PRDX6-Homo-301): 5'-AUUGUAAGCAUUGAUAUCCTT-3'. The siRNA sequence that exhibited the highest interfering efficiency was selected to continue the study. By contrast, one sequence of NC was synthesized as 5'-UUCUCCGAACGUGUCACGUTT-3' (sense), 5'-ACGUGACACGUUCGGAGAATT-3' (antisense). 50 nM PRDX6 siRNAs were transfected into BEAS-2B cells using Lipofectamine 2000 transfection reagent (cat. no. 11668030; Thermo Fisher Scientific, Inc.) at 37˚C with 5% CO_2 for 6 h. All transfections were conducted according to the manufacturer's protocol. After transfection, BEAS-2B cells were cultured at 37˚C with 5% CO_2 in DMEM supplemented with 10% fetal bovine serum and 1% penicillin-streptomycin solution for 48 h, then treated with CSE with/without rapamycin/3-MA.

RNA isolation and reverse transcription-quantitative polymerase chain reaction (RT-qPCR). Total RNA from BEAS-2B cells was isolated using an RNA-Quick Purification Kit (cat. no. RN001; YiShan Biotech) and reverse transcribed into complementary deoxyribonucleic acid (cDNA) using the ReverTra Ace qPCR RT Master Mix (cat. no. FSQ-201; Toyobo Life Science). Briefly, after preparation of RT reaction solution according to the manufacturer's protocols, the reaction solution was incubated at 37˚C for 15 min, heated to 98˚C for 5 min and then stored at 4˚C or -20˚C. Next, 40 ng cDNA was used as a template for the operation of qPCR according to the manufacturer's protocols using the SYBR Green Realtime PCR Master Mix Plus (cat. no. QPK-212; Toyobo Life Science). The primer sequences for PRDX6, TNF-α, IL-1β, IL-6, P16, P21 and β-actin were as follows: PRDX6 forward: 5'-GCATCCGTTTCCACGACT-3'; PRDX6 reverse: 5'-TGCACACTGGGGTAAAGTCC-3'; TNF-α forward: 5'-CTTCTGCCTGCTGCACTTTG-3'; TNF-α reverse: 5'-GTCACTCGGGGTTCGAGAAG-3'; IL-1β forward: 5'-GTACCTGTCCTGCGTGTTGA-3'; IL-1β reverse: 5'-GGGAACTGGGCAGACTCAAA-3'; IL-6 forward: 5'-GAGGAGACTTGCCTGGTGAA-3'; IL-6 reverse: 5'-TGGCATTTGTGGTTGGGTCA-3'; P16 forward: 5'-CTTGGTGACCCTCCGGATTC-3'; P16 reverse: 5'-CCACGAGATGTGAACCACGA-3'; P21 forward: 5'-AGTACCCTCTCAGCTCCAGG-3'; P21 reverse: 5'-TGTCTGACTCCTTGTTCCGC-3'; β-actin forward: 5'-CCAACCGCGAGAAGATGA-3'; and β-actin reverse: 5'-CCAGAGGCGTACAGGGATAG-3'. The amplification cycling

reactions (40 cycles) were performed as follows: 15 sec at 95˚C and 1 min at 60˚C. The relative quantification concentrations of mRNA expression levels in the samples were calculated according to the standard curve and analyzed using the Applied Biosystems QuantStudio 3 Real-Time PCR Systems (cat. no. A28567; Thermo Fisher Scientific, Inc.) at the comparative threshold cycle ($2^{-\Delta\Delta Cq}$) (16).

Western blotting. For each experiment, treated BEAS-2B cells were lysed using RIPA Lysis Buffer (cat. no. P0013B; Beyotime Institute of Biotechnology) supplemented with 1% PMSF; cat. no. ST505; Beyotime Institute of Biotechnology), 1% Phosphatase Inhibitor Cocktail A (EDTA-Free) and 1% Phosphatase Inhibitor Cocktail B (EDTA-Free) (cat. no. M7528; AbMole BioScience) to extract protein. The protein concentration was measured using BCA Protein Assay Kit (cat. no. P0012; Beyotime Institute of Biotechnology) according to the manufacturer's protocol, then 30 μg protein samples were separated on 8-15% gels using SDS-PAGE (cat. no. P0012A; Beyotime Institute of Biotechnology) and then transferred onto a PVDF membrane (cat. no. ISEQ00010; Merck KGaA). The membrane was blocked at room temperature for 15 min using QuickBlock buffer (cat. no. P0220; Beyotime Institute of Biotechnology) and probed with primary antibodies directed against PRDX6 (cat. no. 95336S), P16 (cat. no. 92803S), P21 (cat. no. 2947S), LC3 (cat. no. 2775S), autophagy related 5 (ATG5; cat. no. 2630S), P62 (cat. no. 5114S) and GAPDH (cat. no. 2118S) at 4˚C overnight, which were all used at a dilution of 1:1,000 and purchased from Cell Signaling Technology, Inc. The membrane was then incubated with a specific HRP-conjugated Goat anti-Rabbit IgG secondary antibody (1:1,000; cat. no. 31460; Thermo Fisher Scientific, Inc.) at room temperature for 1 h. The membrane was washed with 0.1% Tween-20 (cat. no. ST825-500ml; Beyotime Institute of Biotechnology) TBST (cat. no. C520009-0500; Sangon Biotech Co., Ltd.) and signals were detected using enhanced chemiluminescence (cat. no. P0018S; Beyotime Institute of Biotechnology). Band densities were quantified using ImageJ 1.46r (National Institutes of Health), and results were normalized by GAPDH and represented as fold change.

Bioinformatics. Using the Gene Expression Omnibus (GEO) database (ncbi.nlm.nih.gov/geo/), the GSE20257 dataset of gene expression profiles based on the GPL570 platform (ncbi.nlm.nih.gov/geo/query/acc.cgi?acc=GPL570), including small airway epithelium samples of 53 healthy non-smokers, 59 healthy smokers and 23 smokers with COPD, was used to explore the potential involvement of PRDX6, autophagy and senescence in COPD (17). Further demographic details of patients from the GSE20257 dataset are presented in Table SI. The dataset was obtained and analyzed using R Studio (RStudio Team, 2021. RStudio: Integrated Development Environment for R; Version 4.1.2, 2021-11-01). The GEO-query (version 2.62.2) package was used to download the GSE20257 mRNA expression profile data and the hgu133plus2.db (version 3.2.3) package was used to find the gene symbols for probes in the raw data. Gene expression profiles were first log2 transformed and then normalized using the 'normalizeBetweenArrays' function in the limma (version 3.50.3) package. Lastly, GraphPad Prism (version 7; Dotmatics) was used to create figures using the data processed with R.

Statistical analysis. Data are presented as the mean ± SD, collected from at least three independent experiments. Unpaired student's t-test was used for the comparison of two datasets, one-way ANOVA followed by Tukey correction was used for the comparison of more than two datasets with one independent variable and two-way ANOVA followed by the Sidak correction was used for the comparison of more than two datasets with two independent variables. Pearson correlation coefficient was used to measure the degree of association between two variables. $P<0.05$ was considered to indicate a statistically significant difference. The statistical software used for analysis was GraphPad Prism (version 7; Dotmatics).

Results

CS exposure reduces PRDX6 levels and induces cellular senescence in the airway epithelial cells of patients with COPD and in vitro. To investigate the possible dysregulation of PRDX6 and senescence during COPD development, the mRNA levels of PRDX6 and senescence markers in the small airway epithelium from patients with COPD in the GSE20257 dataset were examined (Fig. 1A-K). It was revealed that the PRDX6 mRNA levels had a decreasing trend between the non-smoker, smoker and COPD-smoker groups (Fig. 1A). P16 mRNA levels had an increasing trend between the non-smoker, smoker and COPD-smoker groups (Fig. 1B). No significant difference among non-smokers, smokers and patients with COPD was observed for P21 mRNA levels (Fig. 1C). The SIRT1 mRNA level in smokers was significantly lower compared with non-smokers (Fig. 1D). The SIRT6 mRNA level in patients with COPD was significantly lower compared with non-smokers (Fig. 1E).

It was revealed *in vitro* that CSE induced rounding and detachment of BEAS-2B and it was confirmed by microscopy (Fig. 2A), CSE dose- and time-dependently reduced the viability of BEAS-2B cells (Fig. 2B and C). Significant changes in BEAS-2B cells were observed with 1% CSE, further indicated by an increase in the mRNA levels of inflammation factors, TNF-α, IL-1β and IL-6 (Fig. 2D-F). Next, the expression levels of PRDX6 and the senescence markers, P16 and P21, were examined in CSE-treated BEAS-2B cells. PRDX6 mRNA and protein were significantly decreased, while P16 and P21 mRNA were significantly increased in a time-dependent manner, compared with the control group (Fig. 2G-K). P16 and P21 protein levels in the 1% CSE 48 h group were significantly increased compared with that of control group (Fig. 2L-N). However, no significant difference was observed between the 1% CSE 24 h and control groups.

CS exposure induces autophagy dysfunction in the small airway epithelium of smokers, and CSE treatment transiently induces autophagy activation and then induces an autophagy reduction in BEAS-2B cells. To verify the autophagy alteration in COPD, LC3 ATG5 and P62 mRNA levels in the small airway epithelium of non-smokers, smokers and patients with COPD were analyzed. There was no significant difference in the LC3 and ATG5 mRNA levels among the three groups

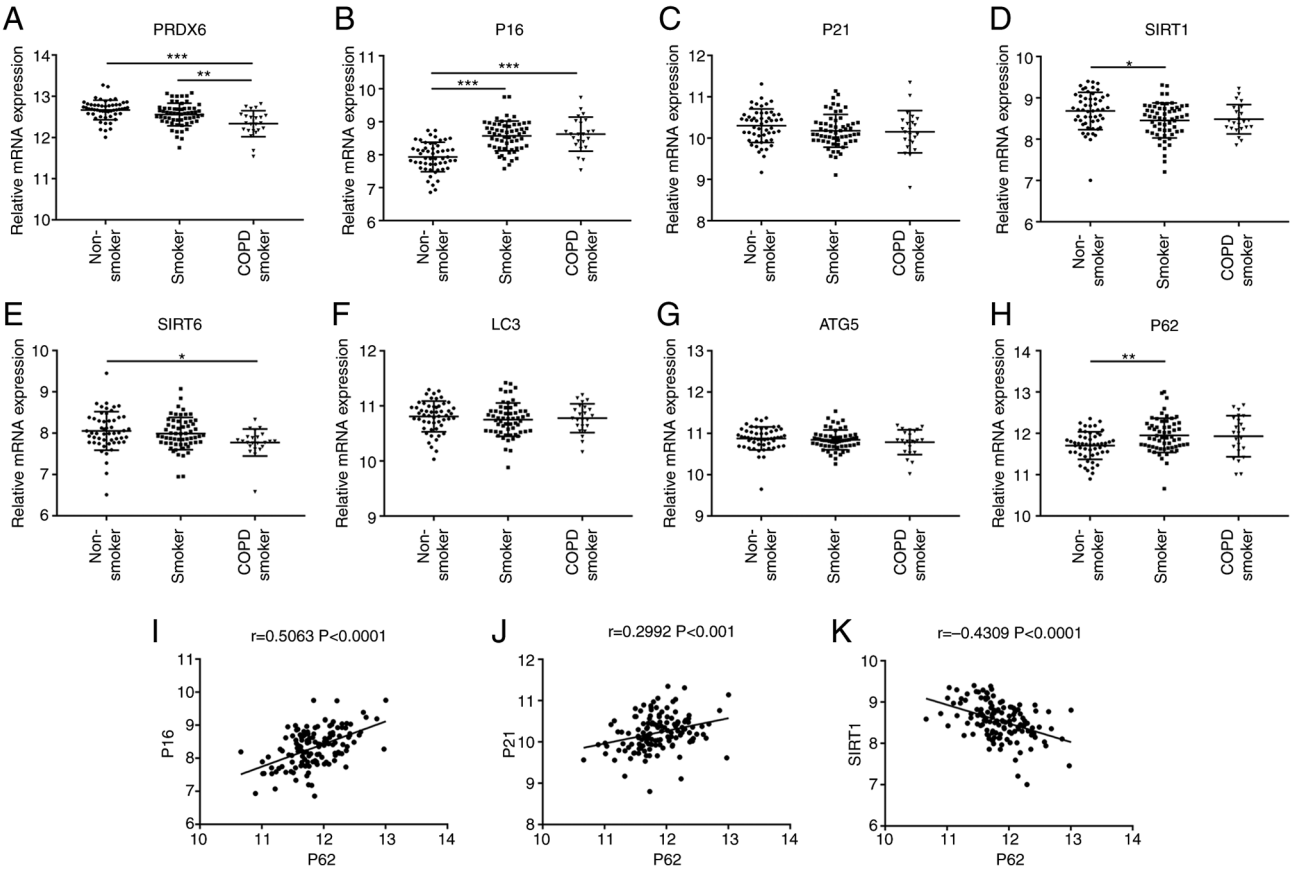

Figure 1. A reduction in PRDX6 level, autophagy dysfunction and accelerated senescence in the small airway epithelium of healthy non-smokers, healthy smokers and COPD-smokers. The gene expression profiles of the GSE20257 dataset from the Gene Expression Omnibus database (ncbi.nlm.nih.gov/geo/) were used to explore the potential involvement of PRDX6, autophagy and senescence in COPD, which included the small airway epithelium samples of 53 healthy non-smokers, 59 healthy smokers and 23 COPD smokers. Datasets were downloaded and analyzed using R Studio (RStudio Team, 2021. RStudio: Integrated Development Environment for R (Version 4.1.2, 2021-11-01). (A) PRDX6, (B) P16, (C) P21, (D) SIRT1, (E) SIRT6, (F) LC3, (G) ATG5 and (H) P62 mRNA expression levels in the healthy non-smoker, healthy smoker and COPD-smoker groups. The correlation analysis of P62 mRNA and (I) P16, (J) P21 and (K) SIRT1 mRNA. *P<0.05, **P<0.01 and ***P<0.001. ATG5, autophagy related 5; PRDX6, peroxiredoxin 6; COPD, chronic obstructive pulmonary disease; SIRT, sirtuin.

(Fig. 1F and G). However, the P62 mRNA level was significantly higher in smokers compared with non-smokers (Fig. 1H). LC3 is a recognized marker of autophagy. When autophagy is activated, LC3-I is gradually transformed into LC3-II, which locates on the membranes of autophagosomes. Therefore, the ratio of LC3 II/I protein is positively correlated with the number of autophagosomes. ATG5 is a key autophagy factor and an integral part of the ATG5-ATG12-ATG16L1 complex that catalyzes the ATG8 lipidation essential for autophagosome formation and expansion. As an autophagy substrate protein, P62 is widely used as an index of autophagy degradation, which is negatively correlated with autophagy. In this study, western blot on LC3 II/I (LC3-II/LC3-I protein ratio, the conversion of LC3 from LC3-I to LC3-II) and ATG5 were performed to evaluate the activation of autophagy, while western blot on P62 was performed to evaluate the degradation of autophagy. *In vitro*, LC3 II/I and ATG5 protein levels in BEAS-2B cells were significantly increased in the 24 h CSE-treated group compared with the control group (Fig. 3A, C and D). However, in the 48 h CSE-treated group, LC3 II/I and ATG5 protein levels were significantly decreased compared with the control group (Fig. 3E, G and H). It was revealed that CSE treatment had an opposite effect on P62 levels (Fig. 3A, B, E and F).

Effects of a reduction in PRDX6 levels on CSE-induced accelerated senescence and autophagy impairment in BEAS-2B cells. Firstly, a PRDX6 knockdown experiment was performed. PRDX6-Homo-233, PRDX6-Homo-301 and PRDX6-Homo-513 siRNA were used to knockdown PRDX6 expression, all of which significantly reduced PRDX6 mRNA levels in BEAS-2B cells compared with the control siRNA group (Fig. 3I). PRDX6-Homo-233 siRNA (for now on termed 'PRDX6 siRNA') was also demonstrated to significantly decrease the PRDX6 protein level compared with the control group (Fig. 3J and K) and was therefore selected for future experiments. P16 and P21 protein levels were both significantly increased in the PRDX6 siRNA group compared with control siRNA group in BEAS-2B cells with or without CSE treatment (Fig. 3L, Q and R). LC3 II/I and ATG5 protein levels were significantly decreased, while P62 was significantly increased in the PRDX6 siRNA group compared with the control siRNA group in CSE-treated BEAS-2B cells (Fig. 3L-O).

PRDX6 knockdown-mediated autophagy impairment is responsible for accelerated cellular senescence in BEAS-2B cells. The involvement of autophagy in

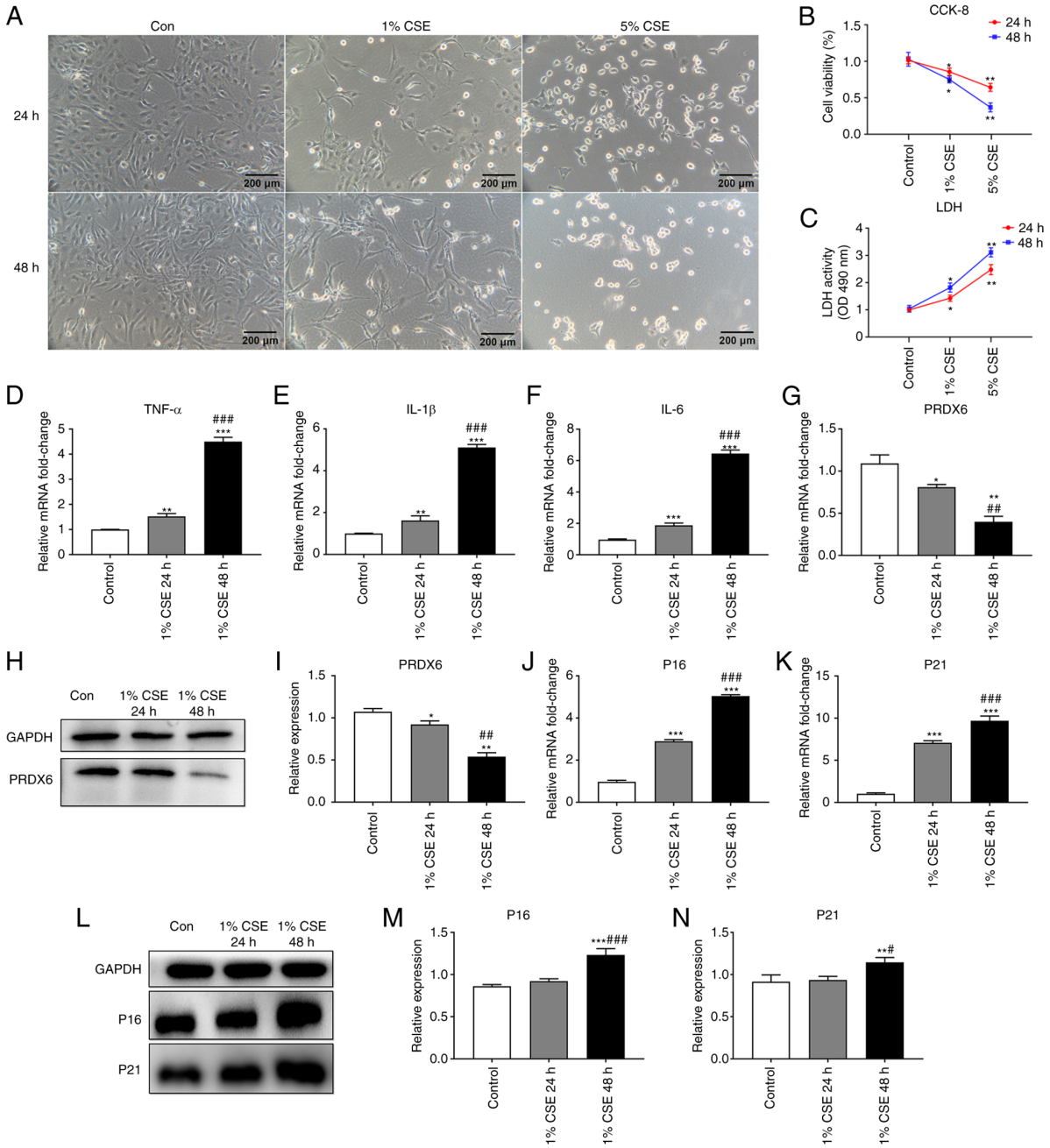

Figure 2. CSE induces a reduction in PRDX6 expression, cellular injury and accelerated senescence in BEAS-2B cells. BEAS-2B cells were treated with 1 and 5% CSE for 24 or 48 h. (A) CSE induced BEAS-2B cell injury (x200 magnification, scale bar 200 μm). CSE induced cellular injury was also observed using (B) cell viability experiments using CCK-8 and (C) cytotoxicity experiments using the LDH assay kit. CSE induced an increase in (D) TNF-α, (E) IL-1β and (F) IL-6 mRNA levels in BEAS-2B cells, when assessed using RT-qPCR. (G) CSE induced a reduction in PRDX6 mRNA levels in BEAS-2B cells, when assessed using RT-qPCR. (H) CSE induced a reduction in PRDX6 levels in BEAS-2B cells when assessed using WB, which was (I) quantified. CSE induced an increase in (J) P16 and (K) P21 mRNA levels in BEAS-2B cells, when assessed using RT-qPCR. β-actin was used as a control for all RT-qPCR experiments when calculating the relative mRNA fold change. (L) CSE induced an increase in (M) P16 and (N) P21 levels in BEAS-2B cells, when assessed using WB. All experiments were reproduced at least three times and performed in triplicate, with bar graphs indicating mean ± SD. *P<0.05, **P<0.01 and ***P<0.001, compared with the control group. $^{\#}$P<0.05, $^{\#\#}$P<0.01 and $^{\#\#\#}$P<0.001, compared with the 1% CSE 24 h group. Con, control; CSE, cigarette smoke extract; PRDX6, peroxiredoxin 6; CCK-8, Cell Counting Kit-8; LDH, lactate dehydrogenase; RT-qPCR, reverse transcription-quantitative polymerase chain reaction; WB, western blotting.

PRDX6 knockdown-mediated accelerated senescence in BEAS-2B cells was next examined. After 48 h of PRDX6 siRNA transfection in BEAS-2B cells, 5 nM rapamycin significantly increased the LC3 II/I protein levels, while it significantly decreased the P62 protein levels, compared with the DMSO-control group (Fig. 4A, B and D). As for ATG5 protein levels, no significant difference was observed between rapamycin and the control group (Fig. 4A, C). Furthermore, the present study demonstrated significantly reduced P16 and P21 protein levels in the rapamycin treated groups compared with the DMSO-control groups with or without CSE treatment (Fig. 4A, E and F). By contrast, 5 mM 3-MA significantly reduced LC3 II/I and ATG5 protein levels, while it significantly increased P62 protein

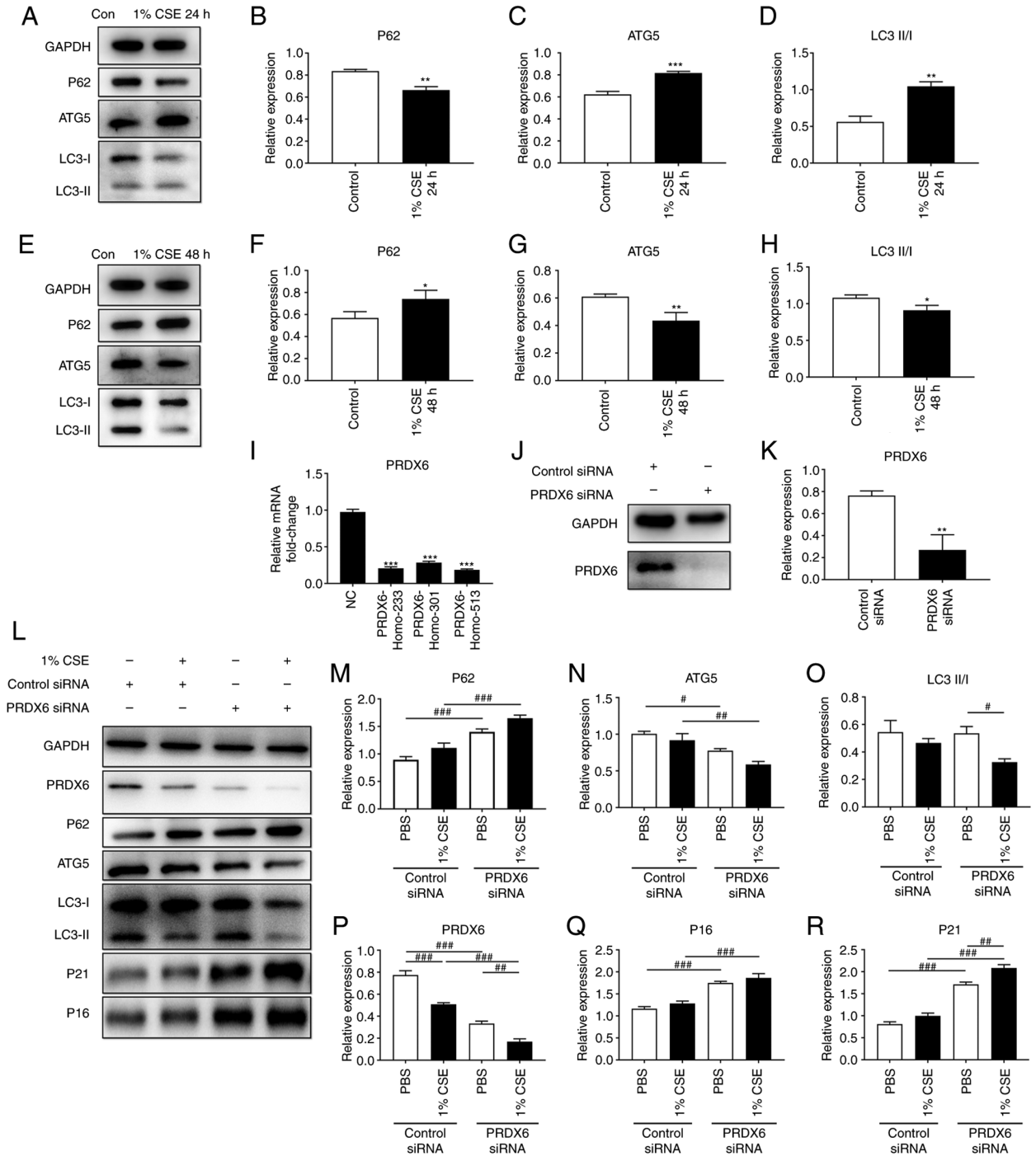

Figure 3. CSE transiently induces autophagy activation, and a reduction in PRDX6 expression aggravates autophagy impairment and accelerates senescence in CSE-treated BEAS-2B. (A) BEAS-2B cells were treated with 1% CSE for 24 h. WB was used to examine and quanitfy (B) P62, (C) ATG5 and (D) LC3 II/I expression levels. (E) BEAS-2B cells were treated with 1% CSE for 48 h. WB was used to examine and quantify (F) P62, (G) ATG5 and (H) LC3 II/I expression levels. PRDX6 knockdown was performed using PRDX6 siRNA and treated for 48 h, to explore the role of PRDX6 in regulating autophagy and senescence in CSE-treated BEAS-2B cells. (I) PRDX6 mRNA levels in BEAS-2B cells after 48 h transfection of PRDX6-Homo-233, PRDX6-Homo-301 and PRDX6-Homo-513 siRNA were examined using RT-qPCR. β-actin was used as the normalization control for all RT-qPCR experiments when calculating relative mRNA fold change. (J) Using WB, PRDX6-Homo-233 was proven to significantly decrease PRDX6 protein levels, which was (K) quanitfied, and thus, PRDX6-Homo-233 was used in further experiments. (L) BEAS-2B cells were treated with 1% CSE for 48 h, following 48 h PRDX6/control siRNA transfection. (M) P62, (N) ATG5, (O) LC3 II/I, (P) PRDX6, (Q) P16 and (R) P21 expression levels were examined using WB and quantified. All experiments were reproduced at least three times and performed in triplicate with bar graphs indicating mean ± SD. *P<0.05, **P<0.01 and ***P<0.001, compared with the NC group, control siRNA group, or control group. $^{\#}$P<0.05, $^{\#\#}$P<0.01 and $^{\#\#\#}$P<0.001 (Sidak correction). ATG5, autophagy related 5; Con, control; CSE, cigarette smoke extract; NC, negative control; PRDX6, peroxiredoxin 6; WB, western blotting; siRNA, small interfering RNA; RT-qPCR, reverse transcription-quantitative polymerase chain reaction.

levels, compared with the PBS control groups (Fig. 4G-J). In addition, P16 protein levels were significantly increased in the 3-MA-treated group compared with the PBS-control group without CSE treatment (Fig. 4G and K). P21 protein

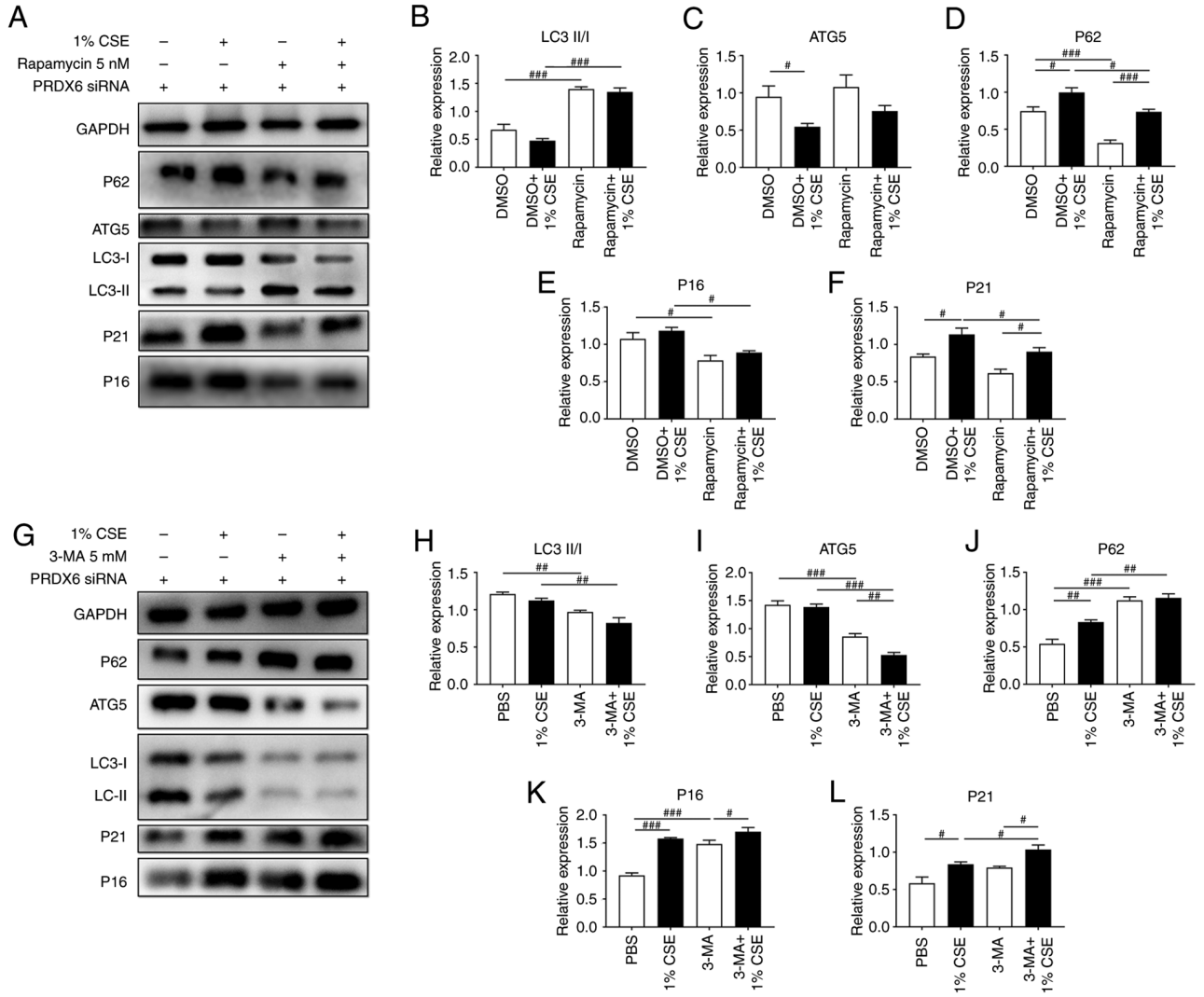

Figure 4. Rapamycin alleviates, while 3-MA aggravates the effect of PRDX6 knockdown on cellular senescence in CSE-treated BEAS-2B. BEAS-2B cells were treated with 1% CSE and 5 nM rapamycin for 48 h, following a 6 h PRDX6 siRNA transfection and 48 h culture. (A) WB was used to examine protein expression levels, which was then quantified for (B) LC3 II/I, (C) ATG5, (D) P62, (E) P16 (F) and P21. BEAS-2B cells were treated with 1% CSE and 5 mM 3-MA for 48 h, following a 6 h PRDX6 siRNA transfection and 48 h culture. (G) WB was used to examine the protein expression levels, which was then quantified for (H) LC3 II/I, (I) ATG5, (J) P62, (K) P16 and (L) P21. All experiments were reproduced at least three times and performed in triplicate with bar graphs indicating mean ± SD. $^{\#}$P<0.05, $^{\#\#}$P<0.01 and $^{\#\#\#}$P<0.001 (Sidak correction). PRDX6, peroxiredoxin 6; 3-MA, 3-Methyladenine; ATG5, autophagy related 5; CSE, cigarette smoke extract; WB, western blotting; siRNA, small interfering RNA.

levels were significantly increased in the 3-MA-treated group compared with the PBS control group with CSE treatment (Fig. 4G and L). Analysis of the GSE20257 dataset demonstrated that P62 mRNA levels were significantly positively correlated with P16 mRNA (r=0.5063, P<0.0001), while weak positively correlated with P21 mRNA (r=0.2992, P<0.001) (Fig. 1I and J). By contrast, P62 mRNA levels showed significant negative correlation with SIRT1 mRNA (r=-0.4309, P<0.0001; Fig. 1K), indicated that insufficient autophagic clearance of damaged proteins could be involved in accelerated cell senescence in COPD.

Discussion

COPD is a global epidemic and has been confirmed as the third leading cause of mortality worldwide and has been recognized as a disease of accelerated lung aging (18,19). Increased cellular senescence is the major feature of aging and it is widely accepted that cellular senescence of airway epithelium plays a crucial role in COPD pathogenesis (20,21). CS-induced autophagy impairment has been demonstrated to be associated with accelerated senescence in COPD (22). The present study focused on cellular senescence and autophagy impairment in COPD, and CSE-induced BEAS-2B cell senescence was performed to mimic the challenge of CS on the airway epithelium of patients with COPD. The present study demonstrated that aging markers, such as P16 and P21, in human airway epithelial cells was significantly increased in patients with COPD and CSE-treated BEAS-2B cells, indicating that accelerated cellular senescence is involved in the pathogenesis of COPD.

PRDX6 is known for its notable antioxidant activity (23). PRDX6 is broadly expressed among tissues especially in lung alveolar type II and Clara cells, and thus plays a crucial role against oxidative stress in the respiratory tract (10). Oxidative

stress is markedly increased in COPD lungs as a result of cigarette smoking or biomass smoke exposure (24). Certain studies have proposed that oxidative damage contributes to the hallmarks of aging, and treatment with antioxidants may prolong lifespan (7,25). Therefore, as an antioxidant, the role of PRDX6 against aging has been previously investigated (12,13). Nevertheless, the role of PRDX6 in airway epithelial cells and in respiratory diseases, such as COPD, remains to be clarified, especially when considering the regulation of PRDX6 in aging or senescence. The present study demonstrated that a reduction in PRDX6 expression could aggravate cellular senescence in CSE-treated BEAS-2B cells. Additionally, PRDX6 knockdown also induced accelerated senescence in BEAS-2B cells in the absence of CSE treatment, suggesting a pivotal role of PRDX6 in regulating cellular senescence in BEAS-2B cells.

Autophagy impairment is proposed to be closely associated to cellular senescence, both of which contribute to the pathogenesis of COPD (26). Nevertheless, whether CSE activates autophagy or induces autophagy impairment in lung epithelial cells remains controversial (22,27,28). Studies showed that different concentrations or durations of CSE treatment result in different outcomes (22,27-37). When considering concentrations of CSE, Vij *et al* (22) found that 10% CSE treatment for 6 h could induce autophagy impairment in BEAS-2B cells, while Wang *et al* (37) found that 1% CSE treatment for 1, 4, 8 and 24 h induced a marked elevation of autophagy in HBE cells. Fujii *et al* (28) found that 1% CSE induced autophagy in HBEC, which peaked 12-24 h after treatment, while was barely detected compared to control group after 36-48 h 1% CSE treatment, indicating that CSE-induced autophagy was transient. In the present study it was assumed that different concentrations or durations of CSE treatment could result in different outcomes, and it was demonstrated that 1% CSE was sufficient to observe significant damage and cellular senescence changes in BEAS-2B cells. Hence, 1% CSE was selected as the standard treatment concentration in further experiments. Previous studies indicated that CSE treatment could activate autophagy. However, CSE treatment in these studies lasted ≤24 h (37,38). The present study hypothesized that extending the duration of CSE treatment could induce autophagy impairment in BEAS-2B cells. Fujii *et al* (28) demonstrated that 1% CSE activates autophagy in HBE cells at 12-24 h and more than triple the level of LC3-II was observed in these cells compared with the control group. The LC3-II level in the CSE treated group was lower than that of the control group at 36-48 h. The present study demonstrated a similar result in BEAS-2B cells, with higher levels of LC3 II/I in the 24 h CSE treatment group and lower levels of LC3 II/I in the 48 h CSE treatment group, compared with the respective control groups. We therefore hypothesize that CSE first induces autophagy activation in BEAS-2B cells, which then plays a defensive role against the toxic components in CSE. Long-term CSE exposure then induces autophagy impairment and even cell death. The present study demonstrated that 1% CSE treatment for 48 h could decrease the level of autophagy in BEAS-2B cells. Therefore, smokers could have a defective autophagy flux compared with non-smokers, which may be related to accelerated senescence and contribute towards COPD progression (22,39).

There were, however, several limitations to the present study. First, the present study only focused on PRDX6 knockdown experiments using siRNA, and PRDX6 overexpression experiments should also be performed. Second, only the commercial human lung epithelial cell line, BEAS-2B, were used in the present study. Further studies with experimental validations using lung tissue homogenate and primary lung epithelial cells of humans and animals are required to validate the roles of PRDX6 in the regulation of autophagy and senescence in COPD. Third, it is necessary to investigate the roles of PRDX6 in specific signaling pathways, such as the PINK1/Parkin pathway, to further examine the mechanisms of PRDX6 in regulating autophagy and senescence in COPD.

In conclusion, during the development of COPD, the expression of PRDX6 is downregulated and autophagy is impaired, which may contribute to an accelerated cellular senescence. A reduction in PRDX6 expression may accelerate senescence, at least in part, though stimulating autophagy impairment in CSE-treated BEAS-2B cells.

Acknowledgements

Not applicable.

Funding

This work was supported by the National Natural Science Foundation of China (grant no. 81970069 and 82170091).

Availability of data and materials

The datasets used and/or analyzed during the current study are available from the corresponding author on reasonable request.

Authors' contributions

The conceptualization and methodology were performed by DY, XW and JL. The investigation and data curation were performed by JL and TW. Validation and formal analysis of the data was performed by JL, KL and CB. The original draft was written by JL, XW and CB. The manuscript was reviewed and edited by XW and DY. Funding was acquired by DY. JL and TW confirm the authenticity of all the raw data. All authors read and approved the final manuscript.

Ethics approval and consent to participate

Not applicable.

Patient consent for publication

Not applicable.

Competing interests

The authors declare that they have no competing interests.

References

1. Momtazmanesh S, Moghaddam SS, Ghamari SH, Rad EM, Rezaei N, Shobeiri P, Aali A, Abbasi-Kangevari M, Abbasi-Kangevari Z, Abdelmasseh M, *et al*; GBD 2019 Chronic Respiratory Diseases Collaborators: Global burden of chronic respiratory diseases and risk factors, 1990-2019: An update from the Global Burden of Disease Study 2019. EClinicalMedicine 59: 101936, 2023.
2. Mannino DM and Buist AS: Global burden of COPD: Risk factors, prevalence, and future trends. Lancet 370: 765-773, 2007.
3. Barnes PJ: New concepts in chronic obstructive pulmonary disease. Annu Rev Med 54: 113-129, 2003.
4. Kumar M, Seeger W and Voswinckel R: Senescence-associated secretory phenotype and its possible role in chronic obstructive pulmonary disease. Am J Respir Cell Mol Biol 51: 323-333, 2014.
5. Tsuji T, Aoshiba K and Nagai A: Cigarette smoke induces senescence in alveolar epithelial cells. Am J Respir Cell Mol Biol 31: 643-649, 2004.
6. Tsuji T, Aoshiba K and Nagai A: Alveolar cell senescence in patients with pulmonary emphysema. Am J Respir Crit Care Med 174: 886-893, 2006.
7. Harman D: Free radical theory of aging: An update: Increasing the functional life span. Ann N Y Acad Sci 1067: 10-21, 2006.
8. Rajawat YS, Hilioti Z and Bossis I: Aging: Central role for autophagy and the lysosomal degradative system. Ageing Res Rev 8: 199-213, 2009.
9. Karplus PA and Hall A: Structural survey of the peroxiredoxins. Subcell Biochem 44: 41-60, 2007.
10. Kim TS, Dodia C, Chen X, Hennigan BB, Jain M, Feinstein SI and Fisher AB: Cloning and expression of rat lung acidic Ca^{2+}-independent PLA2 and its organ distribution. Am J Physiol 274: L750-L761, 1998.
11. Park MH, Jo M, Kim YR, Lee CK and Hong JT: Roles of peroxiredoxins in cancer, Neurodegenerative diseases and inflammatory diseases. Pharmacol Ther 163: 1-23, 2016.
12. Chhunchha B, Singh P, Stamer WD and Singh DP: Prdx6 retards senescence and restores trabecular meshwork cell health by regulating reactive oxygen species. Cell Death Discov 3: 17060, 2017.
13. Pacifici F, Della-Morte D, Piermarini F, Arriga R, Scioli MG, Capuani B, Pastore D, Coppola A, Rea S, Donadel G, *et al*: Prdx6 plays a main role in the crosstalk between aging and metabolic sarcopenia. Antioxidants 9: 329, 2020.
14. Lee DH, Jung YY, Park MH, Jo MR, Han SB, Yoon DY, Roh YS and Hong JT: Peroxiredoxin 6 confers protection against nonalcoholic fatty liver disease through maintaining mitochondrial function. Antioxid Redox Signal 31: 387-402, 2019.
15. Ma S, Zhang X, Zheng L, Li Z, Zhao X, Lai W, Shen H, Lv J, Yang G, Wang Q and Ji J: Peroxiredoxin 6 is a crucial factor in the initial step of mitochondrial clearance and is upstream of the PINK1-parkin pathway. Antioxid Redox Signal 24: 486-501, 2016.
16. Livak KJ and Schmittgen TD: Analysis of relative gene expression data using real-time quantitative PCR and the 2(-Delta Delta C(T)) method. Methods 25: 402-408, 2001.
17. Shaykhiev R, Otaki F, Bonsu P, Dang DT, Teater M, Strulovici-Barel Y, Salit J, Harvey BG and Crystal RG: Cigarette smoking reprograms apical junctional complex molecular architecture in the human airway epithelium in vivo. Cell Mol Life Sci 68: 877-892, 2011.
18. Bai J, Cui J and Yu C: Burden of chronic obstructive pulmonary disease attributable to non-optimal temperature from 1990 to 2019: A systematic analysis from the global burden of disease study 2019. Environ Sci Pollut Res Int 30: 68836-68847, 2023.
19. Barnes PJ: Senescence in COPD and its comorbidities. Annu Rev Physiol 79: 517-539, 2017.
20. Tam A and Sin DD: Senescence in chronic lung diseases: Therapeutic potential disease. Med Clin North Am 96: 681-698, 2012.
21. Adnot S, Amsellem V, Boyer L, Marcos E, Saker M, Houssaini A, Kebe K, Dagouassat M, Lipskaia L and Boczkowski J: Telomere dysfunction and cell senescence in chronic lung diseases: Therapeutic potential. Pharmacol Ther 153: 125-134, 2015.
22. Vij N, Chandramani-Shivalingappa P, Van Westphal C, Hole R and Bodas M: Cigarette smoke-induced autophagy impairment accelerates lung aging, COPD-emphysema exacerbations and pathogenesis. Am J Physiol Cell Physiol 314: C73-C87, 2018.
23. Pacifici F, Della Morte D, Capuani B, Pastore D, Bellia A, Sbraccia P, Di Daniele N, Lauro R and Lauro D: Peroxiredoxin6, a multitask antioxidant enzyme involved in the pathophysiology of chronic noncommunicable diseases. Antioxid Redox Signal 30: 399-414, 2019.
24. Kirkham PA and Barnes PJ: Oxidative stress in COPD. Chest 144: 266-273, 2013.
25. Della-Morte D, Ricordi C and Rundek T: The fountain of youth: Role of sirtuins in aging and regenerative medicine. Regen Med 8: 681-683, 2013.
26. Kuwano K, Araya J, Hara H, Minagawa S, Takasaka N, Ito S, Kobayashi K and Nakayama K: Cellular senescence and autophagy in the pathogenesis of chronic obstructive pulmonary disease (COPD) and idiopathic pulmonary fibrosis (IPF). Respir Investig 54: 397-406, 2016.
27. Chen ZH, Kim HP, Sciurba FC, Lee SJ, Feghali-Bostwick C, Stolz DB, Dhir R, Landreneau RJ, Schuchert MJ, Yousem SA, *et al*: Egr-1 regulates autophagy in cigarette smoke-induced chronic obstructive pulmonary disease. PLoS One 3: e3316, 2008.
28. Fujii S, Hara H, Araya J, Takasaka N, Kojima J, Ito S, Minagawa S, Yumino Y, Ishikawa T, Numata T, *et al*: Insufficient autophagy promotes bronchial epithelial cell senescence in chronic obstructive pulmonary disease. OncoImmunology 1: 630-641, 2012.
29. Miao Q, Xu Y, Zhang H, Xu P and Ye J: Cigarette smoke induces ROS mediated autophagy impairment in human corneal epithelial cells. Environ Pollut 245: 389-397, 2019.
30. Kono Y, Colley T, To M, Papaioannou AI, Mercado N, Baker JR, To Y, Abe S, Haruki K, Ito K and Barnes PJ: Cigarette smoke-induced impairment of autophagy in macrophages increases galectin-8 and inflammation. Sci Rep 11: 335, 2021.
31. Govindaraju VK, Bodas M and Vij N: Cigarette smoke induced autophagy-impairment regulates AMD pathogenesis mechanisms in ARPE-19 cells. PLoS One 12: e0182420, 2017.
32. Xu SW, Zhang YJ, Liu WM, Zhang XF, Wang Y, Xiang SY, Su JC and Liu ZB: Cigarette smoke extract-induced inflammatory response via inhibition of the TFEB-mediated autophagy in NR8383 cells. Exp Lung Res 49: 39-48, 2023.
33. Bodas M, Patel N, Silverberg D, Walworth K and Vij N: Master autophagy regulator transcription factor EB regulates cigarette smoke-induced autophagy impairment and chronic obstructive pulmonary disease-emphysema pathogenesis. Antioxid Redox Signal 27: 150-167, 2017.
34. Pei C, Wang X, Lin Y, Fang L and Meng S: Inhibition of galectin-3 alleviates cigarette smoke extract-induced autophagy and dysfunction in endothelial progenitor cells. Oxid Med Cell Longev 2019: 7252943, 2019.
35. Chen S, Wang Y, Zhang H, Chen R, Lv F, Li Z, Jiang T, Lin D, Zhang H, Yang L and Kong X: The antioxidant MitoQ protects against CSE-induced endothelial barrier injury and inflammation by inhibiting ROS and autophagy in human umbilical vein endothelial cells. Int J Biol Sci 15: 1440-1451, 2019.
36. Hwang JW, Chung S, Sundar IK, Yao H, Arunachalam G, McBurney MW and Rahman I: Cigarette smoke-induced autophagy is regulated by SIRT1-PARP-1-dependent mechanism: Implication in pathogenesis of COPD. Arch Biochem Biophys 500: 203-209, 2010.
37. Wang Y, Liu J, Zhou JS, Huang HQ, Li ZY, Xu XC, Lai TW, Hu Y, Zhou HB, Chen HP, *et al*: MTOR suppresses cigarette smoke-induced epithelial cell death and airway inflammation in chronic obstructive pulmonary disease. J Immunol 200: 2571-2580, 2018.
38. An CH, Wang XM, Lam HC, Ifedigbo E, Washko GR, Ryter SW and Choi AM: TLR4 deficiency promotes autophagy during cigarette smoke-induced pulmonary emphysema. Am J Physiol Lung Cell Mol Physiol 303: L748-L757, 2012.
39. Rabe KF, Hurd S, Anzueto A, Barnes PJ, Buist SA, Calverley P, Fukuchi Y, Jenkins C, Rodriguez-Roisin R, van Weel C, *et al*: Global initiative for chronic obstructive lung disease: Global strategy for the diagnosis, management, and prevention of chronic obstructive pulmonary disease: GOLD executive summary. Am J Respir Crit Care Med 176: 532-555, 2007.